Nonrandom connectivity in local cortical circuits from anisotropic axon morphology

Felix Z. Hoffmann[1,2*], Stefan Rotter[1,3]

1 Bernstein Center Freiburg, Freiburg, Germany
2 Frankfurt Institute for Advanced Studies, Frankfurt am Main, Germany
3 Faculty of Biology, University of Freiburg, Freiburg, Germany

* hoffmann@fias.uni-frankfurt.de

Abstract

Nonrandom connectivity patterns have been repeatedly found in local cortical networks, but it remains unclear which connection principles underlie this form of network organization. Here we present a simple geometric random network model that implements connectivity as one would expect from neuron-typical axon and dendrite morphology. The statistics of are well reproduce in our model. We are able to show that the emerging nonrandomness is indeed due to networks anisotropy in connectivity. Our results show that characteristic neuron morphology must therefore be considered as an important aspect of the connection principles in the cortex.

Suggesting that features of the pyramdial neuron's stereotypical morphology can be the cause for such non-randomness, a simplistic geometric random network model is introduced reflecting "anisotropy in neural connectivity", the observation that synapses of cortical pyramidal cells tend to cluster around the main axon's projection. Analysis of the network's connectivity reveals patterns closely resembling the findings in cortical circuits. Characteristic neuron morphology must therefore be considered as an important aspect of the underlying connection principles in the cortex. Reflecting network non-random network connectivity faithfully, the proposed model offers itself for further investigation of the consequences of patterns consequences in networks dynamics and learning.

Introduction

The network structure has large effect on functional properties of the network such as correlations [1]

Here we turn stereotypical features of the . In general, neuron morphology is highly diverse, ranging from . However, within a neuron type in a specific, morphology can be . Pyramidal cells in the layer 5 show rather (Fig 1).

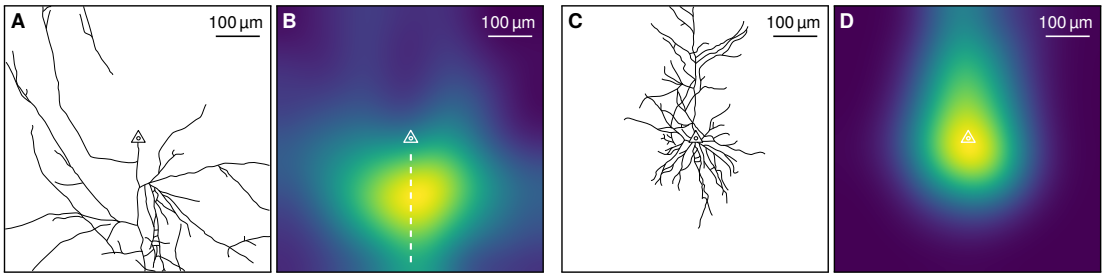

Figure 1: **Anisotropy in stereotypical morphology of layer 5 pyramidal cells**. **A**: Axon reconstruction of thick tufted layer 5 rat somatosensory cortex (P14, retraced from Romand et al. [2]). Triangle symbolizes soma. **B**: Axon branch density heatmap. Five tracings as in A (all retraced from [2]) were overlayed with soma algined in the center and main axon pointing downwards (white dashed line). High branch density (yellow colors) is found along the main axon projection revealing an anisotropy in axon morphology. **C**: As in A, but for dendrite. **D**: Dendrite branch density heatmap obtained as in B. High dendrite branch density is found isotropically around the soma.

Methods

We consider four types of random network models and analyze their connectivity structure. The anisotropic and tuned anisotropic networks are simple models that implement anisotropy in spatial connectivity as motivated from steoreotypical pyramidal cell morphology. The rewired versions of those networks lack anisotropy but can be seen as otherwise equivalent in their connectivity and provide an important reference for this study. The distance-dependent networks allow for further distinction between effects on the network connectivity structure that are direct or indirect consequence of anisotropy.

Anisotropic networks

The anisotropic network model is the simplest form of a random network featuring anisotropy in connectivity. In the model the N nodes of the network are first distributed uniformly at random on a square of side length E. Each node v is randomly assigned an angle $\alpha \in [0, 2\pi)$. Directed connections are then established from v to other nodes with distance less than $\frac{w}{2}$ to the projection ray originating from v with angle α (Fig. 2). We chose $N = 1000$, leaving the ratio $\frac{w}{E}$ as a free parameter of the model determining the connection density of the network. We selected $E = 296\,\mu\text{m}$ and determined $w = 74.6\,\mu\text{m}$ to obtain a connection density of $p = 11.6$ as in [3]. For a formal mathematical definition of the anisotropic network model see supplementary material (S1).

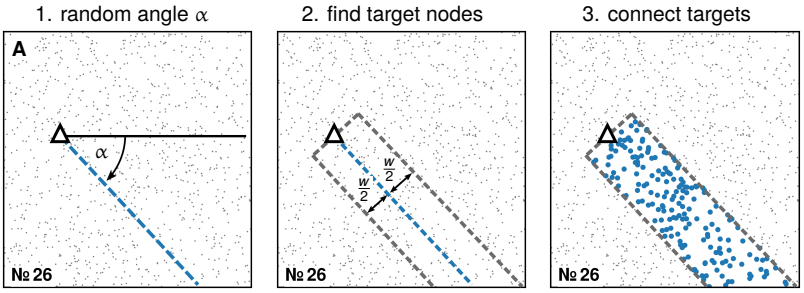

Figure 2: **Anisotropic network model**. **A**: Algorithm for the generation of the network. First the N nodes (grey dots) are distributed randomly on the square surface. Then, for each source node (shown as $\triangle$, identification number in the bottom left corner) a random angle $\alpha \in [0, 2\pi)$ is chosen (1.). The target nodes for $\triangle$ are found within euclidean distance of less than $\frac{w}{2}$ from the projection originating at $\triangle$ in the direction of α (2., projection shown in blue, dashed). Connections are then established from the source to the target nodes (3., targets of $\triangle$ shown in blue, remaining unconnected nodes in grey). **B**: Targets of another node (identification number 54) with different location and projection angle α.

Rewired networks

In order to identify connectivity features that are a direct result of a network's anisotropy in spatial connectivity, we introduce rewired versions of anisotropic networks. In the rewiring process existing edges are randomly assigned new targets so that anisotropy is eliminated while other important connectivity statistics, such as distance-dependent connectivity and in- and out-degree distributions, are preserved. For example, Fig. 3A shows the targets of a node in the original anisotropic network which are to be rewired. The same node is then shown in Fig. 3B with its new targets in the rewired network.

The rewiring algorithm has two parameters – the rewiring fraction η of edges to be rewired and the rewiring margin ε that determines how many rewiring targets are on average available. In

the process any given edge of the graph gets rewired with probability η. If an edge e with source node $s(e)$ and target node $t(e)$ is to be rewired, at first the Euclidean distance x between $s(e)$ and $t(e)$ is recorded. Potential new targets for e are then all nodes that have a distance to $s(e)$ larger than $x - \frac{\varepsilon}{2}$ but smaller than $x + \frac{\varepsilon}{2}$ (Fig. 3E). From the pool of potential new targets are chosen at random until a target is found that does not already receive input from $s(e)$ either through a previously rewired edge or an edge that will not be rewired if $\eta < 1$. The original edge e is then replaced by a new edge e' from $s(e)$ to the new target (Fig. 3F). If no such target is available the edge is discarded and will not appear in the rewired network.

We chose a rewiring margin $\varepsilon/E = 0.05$ to provide a large enough average number of rewiring targets while closely maintaining the distance-depedent connecitivty in the network (see Section S4). A rewired network, if not otherwise specified, refers to a fully rewired version ($\eta = 1$) of the current network.

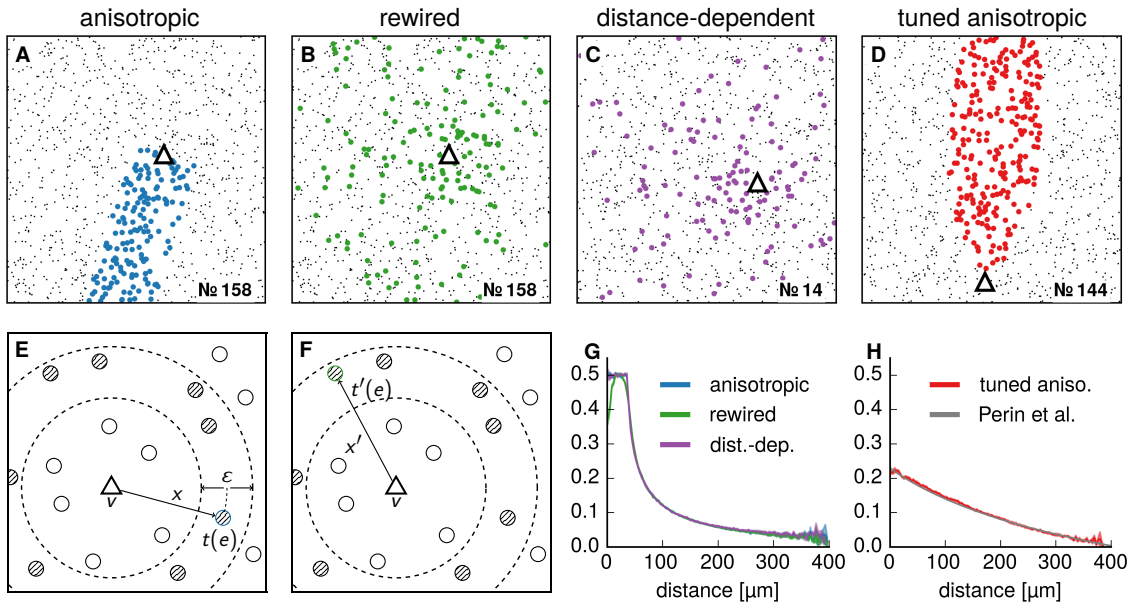

Figure 3: **Overview of network models**. **A**–**D**: Graphic representation of the different network types. For each model the full network area is shown and the $N = 1000$ neuron locations are indicated as gray dots. For a single cell (shown as △, node number indicated in bottom right corner) target nodes of its outgoing connections are marked in color, revealing the typical connectivity in the model. **E**–**F**: Visualization of the rewiring algorithm for a single edge between two neurons (source node v shown as △, target node $t(e)$ hatched in blue) at distance x. First, possible targets within distance $x \pm \varepsilon/2$ are identified (nodes hatched in black). Then, from the pool of possible targets one node is chosen at random as the new target. The rewired edge projects from the original source vertex v to the new target $t'(e)$ (hatched node in green). **G**: Connection probability for a random pair of nodes depends on their inter-node distance. In anisotropic networks (blue) and their rewired versions (green), the distance-depedent connectivity matches. The profile of anisotropic networks was used to generate the distance-dependent networks (purple). **H**: Distance-dependent connection probability profile of the tuned network (red), matched to the findings of Perin et al. [4] (grey).

Distance-dependent networks

A further reference network model are distance-dependent networks. Here, each possible connection is realized independently with a probability $p(x)$, that depends only on the Euclidean distance x between the source and target node (Fig. 3C). We refer to $p(x)$ as the distance-dependent connectivity profile.

Tuned anisotropic networks

Distance-depedent connectivity in anisotropic networks is highly specific (Fig. 3G) and likely not a realistic model for biological systems. In order to obtain distance profiles more closely resembling neural circuit connectivity, we introduce a variation of the anisotropic networks in which w is not fixed, but depends on the distance x from the source node (Fig. 3D). Thus the width w thus becomes a distance-dependent function $w(x)$ in tuned anisotropic networks. We determined $w(x)$ to obtain a distance-dependent connection probability as found by Perin et al. [4] (Fig. 3H, see Section S7 for details). In this case the surface side length $E = 296\,\mu\text{m}$ was picked such that the connection density matched $p = 0.116$ as in Song et al. [3] and the other network types.

Results

We generated samples of anisotropic and tuned anisotropic networks and their respective rewired and distance-dependent versions (see Methods). We analyzed the connectivity structures in these networks and tested which connectivity features emerge from anisotropy in spatial connectivity.

Degree distributions

The number of connections that a node in the network receives (in-degree) or makes to other nodes (out-degree) is an important indicator of the network structure and can strongly affect its dynamics [5, 6]. In our model in-degree distributions in the anisotropic, rewired and distance-dependent networks matched, but were in general broader than the in-degree distribution in random networks of the same connection probability (Fig. 4A-B). Out-degree distributions on the other hand were very broad in anisotropic and rewired networks while distance-dependent networks maintained a distribution similar to the in-degree (Fig. 4C-D). The stretched out distributions in anisotropic networks are a result of some axons being "cut off" at a short length, while other axons travel across the network surface in full length and make numerous connections along the way. The observed difference between in-degree and out-degree distributions in anisotropic networks could be expected in connectomes inferred from slice experiments as well. For this study, we maintain both the distance-dependent and rewired networks as reference models such that features that appear in anisotropic networks but not in rewired and distance-dependent networks can be truthfully attributed to anisotropy in connectivity.

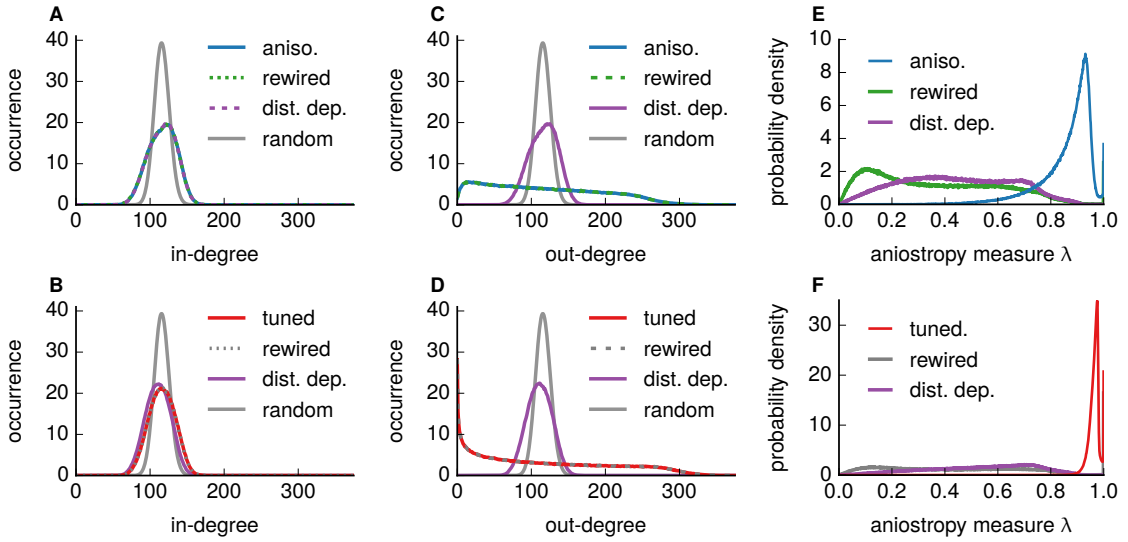

Figure 4: Degree distributions and evaluation of rewiring algorithm **A**: In-degree distribution in anisotropic (blue), rewired anisotropic (green, dashed), distance-dependent (purple, dashed) and random networks (grey). In random networks, a connection between two neurons exists independently with probability p and the in- and out-degree distributions are distributed according to a binomial distribution $B(N, p)$, where $N = 999$ is the number of targets or possible sources for each node. **B**: In-degree distribution in the tuned anisotropic (red), rewired tuned anisotropic (grey, dashed), distance-dependent (purple) and random networks (grey). **C**: Out-degree distribution for networks as in A. **D**: Out-degree distribution for networks as in B. **E**: Probability density distribution of the anisotropy degree λ in the networks, showing that there is strong anisotropy in connectivity in anisotropic networks (blue) but not in rewired (green) or distance-dependent networks (purple). **F**: As in E but for tuned anisotropic (red), rewired tuned anisotropic (grey) and distance-dependent networks (purple).

Rewired networks

Next we to verified that the rewiring algorithm indeed eliminates anisotropy in the network. For this we measured the degree of anisotropy in the targets of a neuron v by summing the normalized vectors pointing from v to its connected target neurons. The resulting vector's norm, divided by the number of targets of v, is then a normalized measure $\lambda(v)$ for the anisotropy in spatial connectivity of v – if target neurons are spread isotropically around the neuron $\lambda(v)$ is close to 0, if almost all targets lie in the same direction from v the value of $\lambda(v)$ is close ton 1 (for a formal definition of λ see supplementary material S8).

Anisotropic and tuned anisotropic networks have distributions of λ with a peak close to 1 (Fig. 4E-F). After rewiring this peak completely vanishes and the distribution of λ in rewired networks approximately matches the distribution in distance-dependent networks. In summary, after rewiring networks have an essentially unchanged equal distance-dependent connectivity (Fig. 3G), maintain the in- and out-degree distribution (Fig. 4A-D) but lack any anisotropy in spatial connectivity that might have been present. With this rewired networks are suitable to test which connectivity features found in anisotropic networks are a direct result of its anisotropy in connectivity.

Two neuron connections

A prominent structure of nonrandom connectivity in cortical circuits is the abundance of reciprocal connections. In networks in which nodes are connected randomly with probability p, such reciprocally connected pairs occur with a low probability of p^2. Experimental results in rat visual cortex [3] and somatosensory cortex [7, 4] however indicate that reciprocally connected pairs of layer 5 pyramidal neurons occur much more often than in a randomly connected network of the same connection density.

We analyzed whether such bidirectionally connected pairs also occur abundantly in anisotropic networks. Indeed, we find that reciprocal connections are overrepresented in both anisotropic in tuned anisotropic networks (Fig. 5A). However, it is yet unclear whether this overrepresentation is a direct result of anisotropy in spatial connectivity. To test this we also determined the occurrence of unconnected, unidirectionally and bidirectionally connected pairs in rewired and distance-dependent networks (Fig. 5B). We found that the different pair motifs occur approximately equally often in the three network types. Reciprocal connections are thus overrepresented in anisotropic, rewired and distance-dependent networks to equal degree.

By construction anisotropic, rewired and distance-dependent networks share the same distance-dependent connection probabilities (Fig. 3G-H). It is thus natural to assume that it is the distance-dependent connectivity in the networks that induces the overabundance of reciprocal connections. Indeed, as connection probabilities within a pair are identical for both directions of connection, an overrepresentation of bidirectional connection is necessarily induced in the network as a result of Jensen's inequality [8]. Is this effect sufficient to explain the experimentally observed overabundance of reciprocal connections? For this we considered the probability of a pair at a given inter-neuron distance to be bidirectionally connected (Fig. 5C-D). While the overall connection probability in tuned anisotropic networks matched the data from Perin et al. [4] (Fig. 5C), the distance-dependent probability for reciprocally connected pairs was much lower than in the experimental results (Fig. 5D). Taken together the results suggest that in cortical circuits organization principles that go beyond anisotropy in connectivity drive the overrepresentation of bidirectional connections. Possible candidates for this are for example synapse dynamics that support bidirectional connections [9] or any other neuron attributes that might affect connection probabilities in a pair-symmetric manner [8, 10].

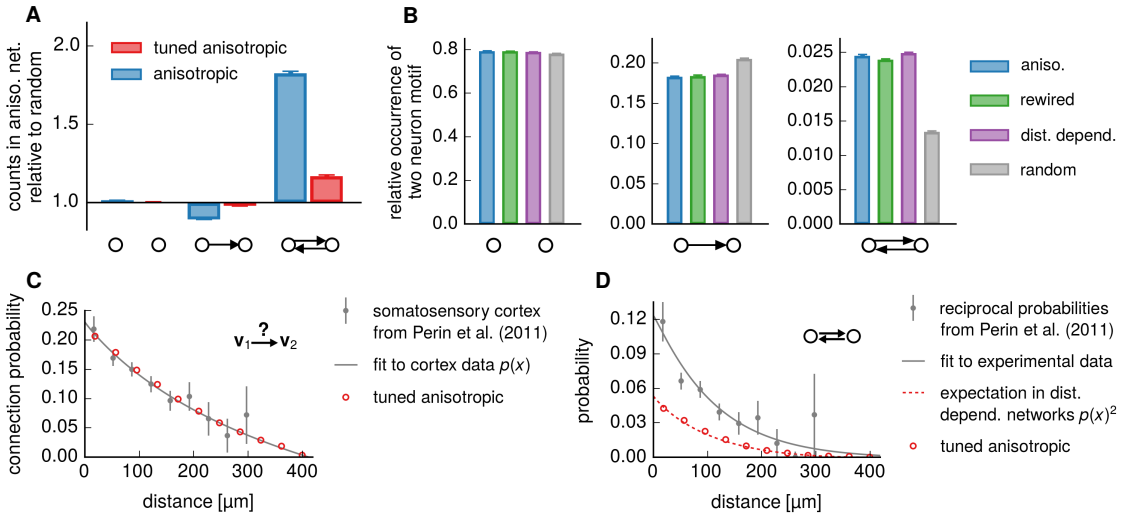

Figure 5: Overrepresentation of reciprocal connections **A**: In anisotropic (blue) and tuned anisotropic networks (red) occurrences of unconnected, unidirectionally and bidirectionally pairs were counted and these values were divided by an expected count of $N(N-1)(1-p)^2$ for unconnected, $N(N-1)p(1-p)$ for unidirectionally connected and $N(N-1)p^2$ for reciprocally connected pairs. Here $p = 0.116$ is connection density in all network types. Reciprocally connected neuron pairs are overrepresented in both anisotropic and tuned anisotropic networks. **B**: Overrepresented reciprocal pairs also occur in rewired and and distance-dependent networks. For unconnected (left), unidirectionally connected (middle) and bidirectionally connected pairs (right), the relative count. While general overrepresentation is found, no significant difference to the rewired mode is identified **C:** Distance-dependent connection probability in tuned anisotropic networks (red) is matching the connection probabilities of layer 5 pyramidal cell in rat somatosensory cortex (grey) as found by Perin et al. [4]. **D:** Distance-dependent probabilities for reciprocal connections is much lower in tuned anisotropic (red circles) than in experimental data (grey) and matches the probabilities expected from C under the assumption of independent realization of connections (red dashed line).

Three neuron motifs

Multiple paired whole-cell recordings in slices of rat visual and somatosensory cortex revealed nonrandom structures in networks of layer 5 pyramidal cells going beyond pair connections – the connection motifs occurring in groups of three neurons deviate significantly of what one would predict from the statistics of connections in neuron pairs [3, 4]. Song et al. for example found the probability for a neuron pair (u, v) to have a connection $u \to v$ to be $p_{u\to v} = 0.0615$ and the probability for a bidirectional connection was $p_{u\leftrightarrow v} = 0.0542$. Form this they computed the probability for a group of three randomly selected neurons to show, for example, the connection motif 14 as labelled in Fig. 6A. The probability was computed as $p_{14} = 3\, p_{u\to v}^2\, p_{u\leftrightarrow v}$, where the factor of 3 is the number of possible ways to arrange the pair connections to obtain the motif (for details and combinatorics of all patterns see supplementary material S9). The actual occurrence of motifs in their data, however, differed significantly from this computed expectation. For example, Song et al. found that motif 14 occurred approximately 3 (± 2) times more often than expected. Other experimental studies [4, 11] and recent computational studies [12, 13] have corroborated the specific occurrence of three neuron patterns in cortical circuits.

Here we analyzed the counts of triplet motifs in anisotropic networks and compared it with the expected counts predicted from pair statistics. We found a highly specific distribution of over- and underrepresented three neuron motifs in anisotropic (Fig. 6A) and tuned anisotropic networks (Fig. 6B), resembling the experimental results of Song et al. [3]. Notably, deviation from the expected counts was in general much lower in rewired and distance-dependent versions of the networks. Indeed, networks with anisotropy in spatial connectivity have significantly over- and underrepresented motifs compared to rewired networks. We found the strongest overrepresentation in anisotropic and tuned networks relative to rewired networks in motifs 10, 12, 14 an 15 (Fig. 6, Fig. S10). This is in good match with the data of Perin et al. [4] who reported motifs 4, 10, 12 and 14 to be overrepresented (motif labels marked with *).

Interestingly motif 4, while generally overrepresented in anisotropic networks, is occurring even more frequently after rewiring. We wondered whether this could be a temporary effect of the rewiring algorithm that would dissipate with repeated rewiring. No such effect was found, distributions remained stable after 5 and 10 repeated runs of the rewiring algorithm on the network (Fig. S11). Taken together the data show that anisotropy in spatial connectivity strongly affects the relative occurrence of three neuron connection patterns. Motifs that are reported to be overrepresented in cortical circuits occur with higher than expected frequency in circuits with anisotropy. This effect is significantly lessened once anisotropy is eliminated, pointing towards the significance of morphology induced anisotropy in shaping the nonrandom connectivity structure of neuronal circuits.

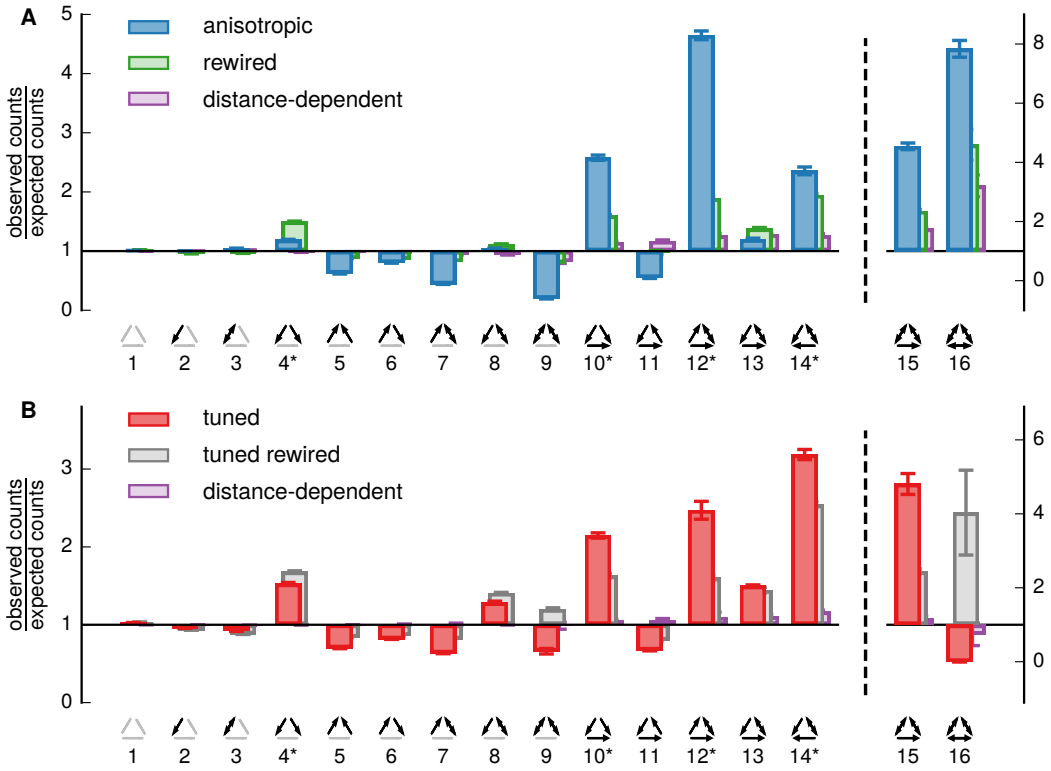

Figure 6: Anisotropy in connectivity induces overrepresentation of specific three neuron motifs. **A**: The ratio between observed triplet motif counts and counts expected from neuron pair connectivity is shown for anisotropic (blue), rewired (green) and distance-dependent networks (purple). Of each network type 5 network instances were created (see Methods for parameters). From each network we sampled $n = 300000$ random groups of three neurons and recorded which of the motifs 1-16 they belong to. The counts for each motif was then divided by the number of occurrences expected from neuron pair probabilities (see S9 for details). Errorbars indicate SEM. Motifs labelled with * were reported by Perin et al. [4] to be overrepresented in layer 5 pyramidal cell of rat somatosensory cortex. **B**: Motif count overrepresentation as in A, here for tuned anisotropic networks (red) and their rewired (grey) and distance-dependent versions (purple).

Neuron clusters

In a study in rat somatosensory cortex, Perin et al. [4] reported nonrandom connectivity patterns of layer 5 pyramidal cells that were not explained by distance-dependent connectivity. Using multiple whole recording the number of connections occurring in groups of up to 12 neurons was recorded. Densely connected clusters occurred much more frequently than expected from distance-dependent connectivity in the slice.

Here we performed a similar analysis. Does anisotropy in spatial connectivity have an effect on the number of connections in neuron clusters? In groups of 3, 6, 8 and 12 randomly selected neurons we counted the number of connections in anisotropic and tuned anisotropic networks as well as in their rewired versions. We found that high counts of connections appear much more frequently in networks with anisotropy than in rewired networks (Fig. 7). Notably, the effect does not seem to be sensitive to the way anisotropy in spatial connectivity was implemented as overrepresentation was approximately equal in anisotropic and tuned anisotropic networks.

As comparison is rewired we find a strong effect due to anisotropy in spatial connectivity that resembles experimental results. However, we asked whether furthing rewiring might introduce . Indeed we observe a small effecct, that is however negible on the scale of the results.

PARAGRAPH how important this is, close that the effect is even stronger comparing with distance-dependent!

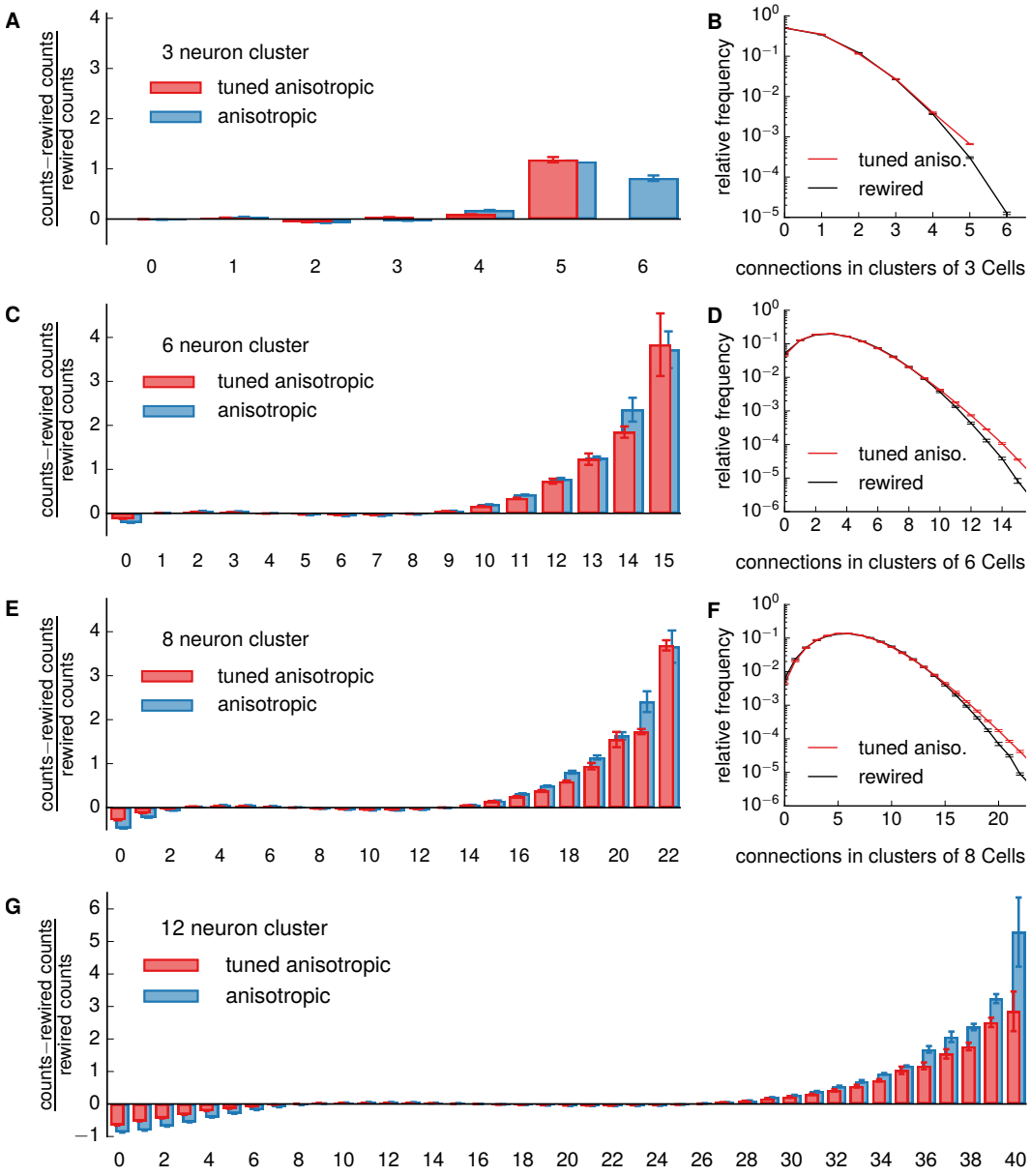

Figure 7: Densely connected groups of neurons appear more frequently in networks with anisotropy. **A**: In anisotropic (blue) and tuned anisotropic networks (red) we sampled $n = 2.5 \times 10^6$ groups of 3 neurons and counted the connections within each group. This process was then repeated for the rewired anisotropic and tuned anisotropic networks. For each number of connections, we plotted the difference between occurrences of this connection count in random groups in anisotropic and rewired networks, divided by the number of occurrences in rewired networks. Fully connected groups did not occur in tuned anisotropic networks. **B**: Relative frequency of number of connections occurring in groups of 3 neurons in tuned anisotropic (red) and rewired tuned anisotropic network (black). **C-D**: As in A-B for groups of 6 neurons. **E-F**: As in A-B for groups on 8 neurons. **G**: As in A for groups of 12 neurons.

Common Neighbor relations

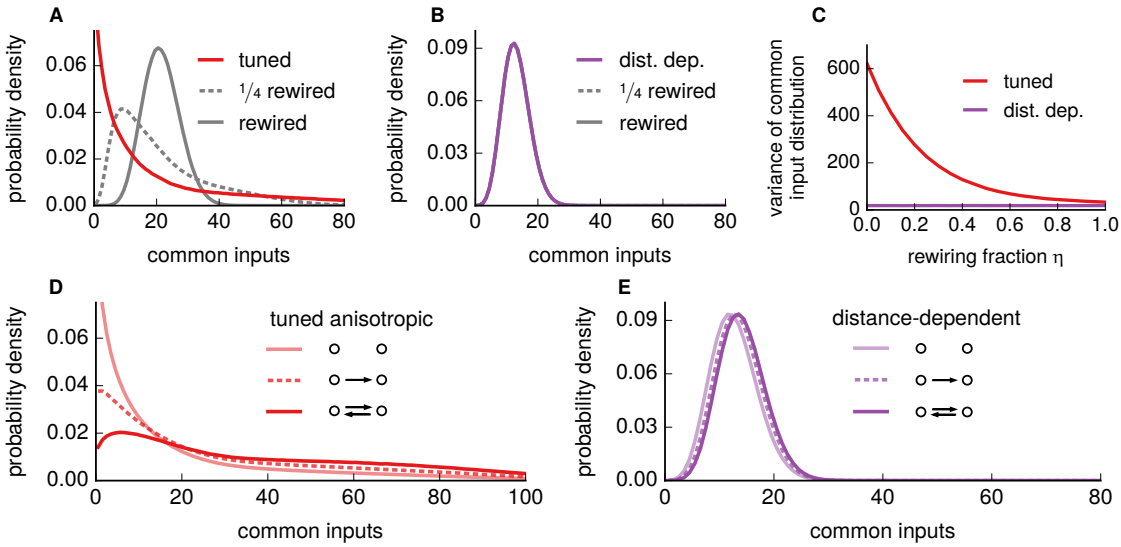

Figure 8: none

Discussion

In this study we analyzed how connectivity might form from the principal of anistropy in spatial connectivity.

Predictions

1. input and output distributions broader than random networks
2. in slice connectomes output distributions measured broader than input distributions

- two neuron not from anisotropy

Acknowledgments

References

[1] V. Pernice, B. Staude, S. Cardanobile, and S. Rotter. How Structure Determines Correlations in Neuronal Networks. In: *PLoS Comput Biol* 7.5 (2011), e1002059. DOI: 10.1371/journal.pcbi.1002059.

[2] S. Romand, Y. Wang, M. Toledo-Rodriguez, and H. Markram. Morphological Development of Thick-Tufted Layer V Pyramidal Cells in the Rat Somatosensory Cortex. In: *Frontiers in Neuroanatomy* 5 (2011). DOI: 10.3389/fnana.2011.00005.

[3] S. Song, P. J. Sjöström, M. Reigl, S. Nelson, and D. B. Chklovskii. Highly Nonrandom Features of Synaptic Connectivity in Local Cortical Circuits. In: *PLoS Biol* 3.3 (2005), e68. DOI: 10.1371/journal.pbio.0030068.

[4] R. Perin, T. K. Berger, and H. Markram. A Synaptic Organizing Principle for Cortical Neuronal Groups. In: *Proceedings of the National Academy of Sciences* 108.13 (2011), pp. 5419–5424. DOI: 10.1073/pnas.1016051108.

[5] A. Roxin. The Role of Degree Distribution in Shaping the Dynamics in Networks of Sparsely Connected Spiking Neurons. In: *Frontiers in Computational Neuroscience* 5 (2011). DOI: 10.3389/fncom.2011.00008.

[6] M. B. Martens, A. R. Houweling, and P. H. E. Tiesinga. Anti-Correlations in the Degree Distribution Increase Stimulus Detection Performance in Noisy Spiking Neural Networks. In: *Journal of Computational Neuroscience* 42.1 (2017), pp. 87–106. DOI: 10.1007/s10827-016-0629-1.

[7] H. Markram, J. Lübke, M. Frotscher, A. Roth, and B. Sakmann. Physiology and Anatomy of Synaptic Connections between Thick Tufted Pyramidal Neurones in the Developing Rat Neocortex. In: *The Journal of Physiology* 500.Pt 2 (1997), pp. 409–440.

[8] F. Z. Hoffmann and J. Triesch. Nonrandom Network Connectivity Comes in Pairs. In: *Network Neuroscience* 1.1 (2017), pp. 31–41. DOI: 10.1162/NETN_a_00004.

[9] C. Clopath, L. Büsing, E. Vasilaki, and W. Gerstner. Connectivity Reflects Coding: A Model of Voltage-Based STDP with Homeostasis. In: *Nature Neuroscience* 13.3 (2010), pp. 344–352. DOI: 10.1038/nn.2479.

[10] W.-C. A. Lee, V. Bonin, M. Reed, B. J. Graham, G. Hood, et al. Anatomy and Function of an Excitatory Network in the Visual Cortex. In: *Nature* (2016). DOI: 10.1038/nature17192.

[11] S. Rieubland, A. Roth, and M. Häusser. Structured Connectivity in Cerebellar Inhibitory Networks. In: *Neuron* 81.4 (2014), pp. 913–929. DOI: 10.1016/j.neuron.2013.12.029.

[12] D. Miner and J. Triesch. Plasticity-Driven Self-Organization under Topological Constraints Accounts for Non-Random Features of Cortical Synaptic Wiring. In: *PLOS Computational Biology* 12.2 (2016). Ed. by O. Sporns, e1004759. DOI: 10.1371/journal.pcbi.1004759.

[13] E. Gal, M. London, A. Globerson, S. Ramaswamy, M. W. Reimann, et al. Rich Cell-Type-Specific Network Topology in Neocortical Microcircuitry. In: *Nature Neuroscience* 20.7 (2017), pp. 1004–1013. DOI: 10.1038/nn.4576.